



Proc. 47nd European Microwave Conference (EuMC)

## MIMO backscatter channel and data transmission measurements

E. Denicke  
H. Hartmann  
B. Geck  
D. Manteuffel

### Suggested Citation:

E. Denicke, H. Hartmann, B. Geck, and D. Manteuffel. MIMO backscatter channel and data transmission measurements. In *Proc. 47nd European Microwave Conference (EuMC)*, pages 723–726, Oct. 2017.

---

This is an author produced version, the published version is available at <http://ieeexplore.ieee.org/>

©2017 IEEE Personal use of this material is permitted. Permission from IEEE must be obtained for all other uses, in any current or future media, including reprinting/republishing this material for advertising or promotional purposes, creating new collective works, for resale or redistribution to servers or lists, or reuse of any copyrighted component of this work in other works.

# MIMO Backscatter Channel and Data Transmission Measurements

Eckhard Denicke, Henning Hartmann, Bernd Geck, Dirk Manteuffel  
Institute of Microwave and Wireless Systems, Leibniz Universität Hannover  
Appelstr. 9A, 30167 Hannover, Germany  
Email: denicke@hft.uni-hannover.de

**Abstract**—Backscatter modulation is more and more establishing itself as an approach for low-cost and low-power data transmission. Combined with multi-antenna techniques and channel state information (CSI) an enhancement of range, reliability or spectral efficiency is achieved. However, there has been few literature about gaining CSI for the individual sub-channels of forward and backward link. The contribution at hand deals with multi-antenna backscatter measurements with up to two scatter antennas and two receive antennas, in order to investigate the backscatter channel and the data transmission within a multipath environment at 5.8 GHz. The paper provides a method for determining the individual sub-channels and investigates the multi-antenna backscatter channel capacity and symbol error ratios for backscatter spatial multiplexing using CSI.

## I. INTRODUCTION

Radio frequency identification (RFID) systems have spread widely into the daily life. Such systems usually employ the principle of backscatter modulation, which is based on transmitting data by modulating the scattering behaviour of a passive (battery-less) or semi-passive (battery-assisted) transponder/tag being interrogated by a reader [1]. Besides its original task of the identification of goods, this technology is used as well in new fields like the internet of things [2], sensing applications, e.g., for medical purposes like neurorecording [3] or in wireless sensor networks [4]. In these fields low-cost and low-power devices are incorporated, demanding increased transponder communication capabilities.

While multiple-input multiple-output (MIMO) techniques in classical communication systems based on, e.g., WiFi or Long-Term Evolution standards are well established, the use of multiple antennas in backscatter systems for transmission or reception at the reader and scattering or reception at the transponder is rather new. Multi-antenna backscatter systems may incorporate  $M$ ,  $L$  and  $N$  antennas at the transmitter (TX), the tag and the receiver (RX), respectively, and span a forward and a backward channel [5]. First concepts for this emerged in 2001 [6], followed by more intensified research in recent years adapting transmission techniques like, e.g., space time coding at the tag end [7].

Wireless MIMO communication systems heavily depend on the properties of the propagation channel in order to achieve the intended enhancement of range, reliability or spectral efficiency. This dependence is even more crucial for backscatter based systems due to their dyadic channel structure, in which fading effects are more severe due to the keyhole nature of

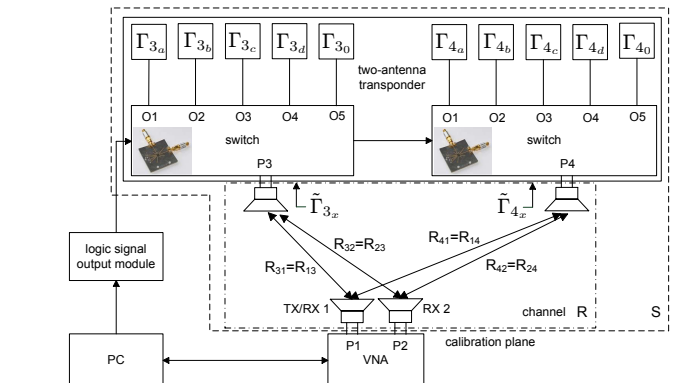


Fig. 1. Scheme of the measurement setup

the propagation paths [5]. Thus, modelling and characterizing the channel is of high importance in order to understand and improve communication theoretic metrics like capacity and error ratios [6] or wireless power transfer aspects [8] of multi-antenna backscatter systems.

Channel state information (CSI) of the individual sub-channels of forward and backward link is essential for achieving optimal performance in terms of power transfer from reader to tag [8] or for advanced communication signaling methods [6], [9]. So far, literature has dealt mainly with channel or fading measurements of the dyadic propagation link in its entirety, i.e., of the product of forward and backward channel including transponders [10]–[12], or with the investigation of backscatter links built in post-processing from traditional one-way channel measurements [13]. In [14] a method for product channel estimation in case of multiple tags and a reader with one transmit and multiple receive antennas is proposed.

However, there has been few literature regarding gaining CSI for the individual sub-channels of forward and backward link. Backscatter transponders are usually hardly able to contribute to the channel estimation due to their energy and hardware limitations, making this task challenging [15]. In this context, the contribution at hand deals with multi-antenna backscatter measurements with up to two scatter antennas and two receive antennas, one of which is used for transmitting as well ( $1 \times 2 \times 2$  system with 1 TX/RX antenna, see [5], [16]). The setup comprises a vector network analyzer (VNA) and a prototype transponder with two scattering antennas (see Fig. 1). The backscatter channel and the transponder data transmission within a multi-path environment are investigated

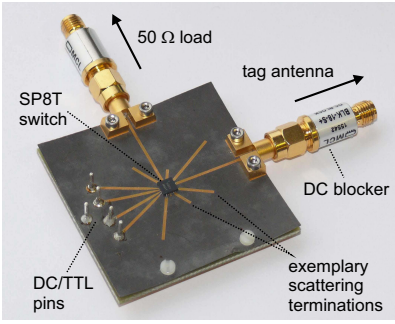


Fig. 2. 4-QAM modulator

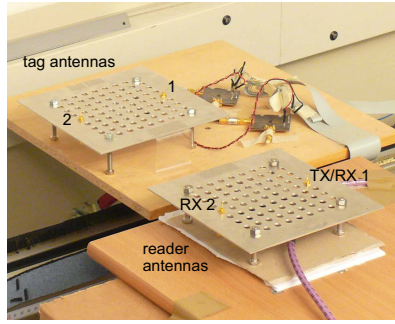


Fig. 3. Tag and reader antennas

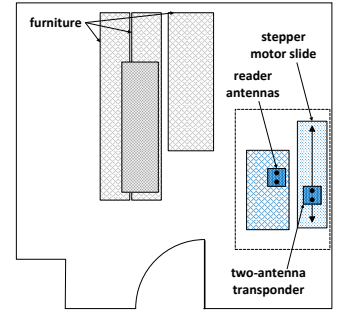


Fig. 4. Measurement site

at 5.8 GHz for a multitude of channel realizations. The paper provides results for the individual sub-channels and investigates the backscatter channel capacity and symbol error ratios for backscatter spatial multiplexing using CSI. Comparable results have not been shown in literature before.

The paper is organized as follows. Sec. II introduces the reader and transponder hardware and describes the measurement scenario. Sec. III presents the signal processing regarding channel estimation, structure of the backscatter signals, capacity calculation and payload detection. Sec. IV discusses the measurement results in terms of channels, capacity and symbol error ratios. The paper is concluded in Sec. V.

## II. MEASUREMENT SETUP

The measurement setup, depicted as a scheme in Fig. 1, is based on a VNA (Rohde & Schwarz ZVA8), which is utilized as a multi-channel vector signal analyzer. The setup constitutes a  $1 \times 2 \times 2$  backscatter system with 1 TX/RX antenna, using two VNA ports, i.e., two antennas for reception, one of which is used as well for transmitting the continuous wave (CW) signal at 5.8 GHz, being backscatter modulated by the two-antenna transponder. This leads to a 4-port scattering matrix  $R$  incorporating the narrowband channel coefficients  $R_{xy}$  being terminated by the scattering coefficients  $\tilde{\Gamma}_{l_x}$  as seen from the tag antenna ports ( $l$  is the scattering port number). For all antennas, monopoles are used. The resulting time-varying 2-port scattering matrix  $S$  is measured over time and post-processed in MATLAB ( $S_{22}$  is not obtained). By this means the data transmission on the backscatter link can be assessed. No modulated reader query signal is necessary, since an experimental transponder is used, triggered via cables. The transponder comprises two monopole antennas connected to two backscatter modulators (asymmetric 4-QAM), realized with open ended microstrip transmission lines of different lengths, connected to a SP8T microwave switch (Hittite HMC321LP4), controlled via TTL with a logic signal output module (Rigol DG-POD-A) [16]. Fig. 2 depicts one of the manufactured modulators. The positioning of modulators and tag antennas relative to the reader antennas is shown in Fig. 3.

The setup is established within a shielded room with some furniture (see Fig. 4), resulting in a multi-path environment incorporating non-line of sight (NLOS) and line-of-sight (LOS)

propagation paths. By positioning the transponder on top of a stepper motor slide, various channel realization are obtained.

## III. SIGNAL PROCESSING

### A. Channel Reconstruction Algorithm

The channel matrix of a  $1 \times 2 \times 2$  system with 1 TX/RX antenna is definable by a reciprocal 4-port scattering matrix  $R$  (see Fig. 1). By terminating two ports of  $R$  with the transponder reflection loads, the measurable 2-port-scattering matrix is

$$S = \begin{pmatrix} S_{11} & S_{12} \\ S_{21} & S_{22} \end{pmatrix} = \begin{pmatrix} R_{11} & R_{12} \\ R_{21} & R_{22} \end{pmatrix} + \begin{pmatrix} R_{13} & R_{14} \\ R_{23} & R_{24} \end{pmatrix} \cdot \left( \begin{pmatrix} \tilde{\Gamma}_{3_x} & 0 \\ 0 & \tilde{\Gamma}_{4_x} \end{pmatrix}^{-1} - \begin{pmatrix} R_{33} & R_{34} \\ R_{43} & R_{44} \end{pmatrix} \right)^{-1} \cdot \begin{pmatrix} R_{31} & R_{32} \\ R_{41} & R_{42} \end{pmatrix}. \quad (1)$$

In order to determine the desired channel information, one out of three loads of the transponder signaling matrix is used as a known termination  $\tilde{\Gamma}_{l_x}$  for each tag antenna at one time, while the other tag antenna is terminated with the reference impedance of  $50 \Omega$  ( $\tilde{\Gamma}_{l_0} \approx 0$ ). By this means (1) simplifies to

$$S_{nm_{a,b,c}} = R_{nm} + \frac{R_{lm}R_{nl}\tilde{\Gamma}_{l_{a,b,c}}}{1 - R_{ll}\tilde{\Gamma}_{l_{a,b,c}}}, \quad (2)$$

where  $m$  denotes the transmitting and  $n$  the receiving port number. By measuring  $S$  in  $L \cdot 3 = 2 \cdot 3 = 6$  transponder states, the relevant parts of  $R$  can be calculated in accordance to the three-term error model (see [16], [17]), comparable to characterizing a multi-port scattering matrix with a VNA using a reduced number of ports. Consequently, a corresponding training symbol sequence is scattered by the transponder as a preamble prior to the payload symbols.

### B. Structure of the Data Signal

For each position of the stepper motor slide, i.e., for each distinct static channel realization, spatially multiplexed random payload data is scattered, headed by a preamble. The preamble consists of 1 symbol used for triggering purposes, 12 constant symbols utilized for noise estimation and 24 training symbols. The latter comprises 8 symbols for channel estimation (6 are used, see Sec. III-A) and  $4^{L=2} = 16$  reference symbols used for data detection (both modulators scatter at the same time in all combinations appearing like a 16-QAM, cp.

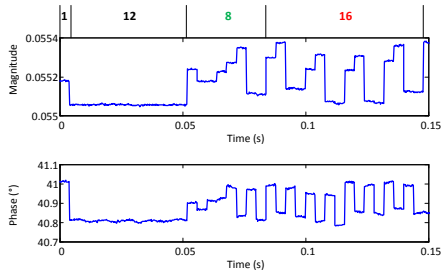


Fig. 5. Exemplary scattering parameter  $S_{11}$  (over time)

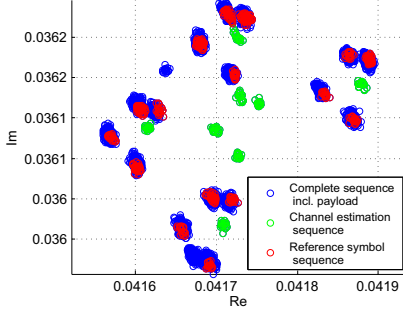


Fig. 6. Exemplary scattering parameter  $S_{11}$  (I/Q)

Sec. III-D2). Fig. 5 and Fig. 6 show, exemplarily, the measured scattering parameter  $S_{11}$  over time and as the corresponding constellation diagram for one channel realization.

### C. Channel Capacity

The capacity of the backscatter link is affected by both the forward and the backward channel [6]. The forward channel accounts for power delivery to the tag antennas for energy harvesting and backscattering, whereas the backward channel depends on a rich scattering scenario to achieve significant capacity. The channel capacity is calculated as follows [18]:

$$C = \log_2(\det[\mathbf{I} + \rho \mathbf{H}_b \mathbf{H}_f \mathbf{Q} \mathbf{H}_f^H \mathbf{H}_b^H]) , \quad (3)$$

with  $\mathbf{Q} = E[\mathbf{x}\mathbf{x}^H]$ .

$\mathbf{H}_f = \begin{pmatrix} R_{31} \\ R_{41} \end{pmatrix}$  and  $\mathbf{H}_b = \begin{pmatrix} R_{13} & R_{14} \\ R_{23} & R_{24} \end{pmatrix}$  are the forward and backward channel matrices, i.e., the respective sub-matrices of  $\mathbf{R}$ . The signal-to-noise ratio (SNR) is denoted by  $\rho$ ,  $\mathbf{x}$  is the reader CW transmit signal,  $\mathbf{H}$  is the Hermitian transpose operator and  $E$  is the expectation. The magnitude of the CW signal and the backscatter symbols is supposed to be unity.

### D. Detection of the Transponder Payload Data

1) *Zero Forcing*: In order to detect the backscatter payload data in MATLAB post-processing, a zero forcing equalizer was implemented (modified from [9]). By this means both symbol streams are separated from each other using CSI gained from the preamble. An independent symbol decision is made and the symbol error ratio (SER) is determined.

2) *Reference Symbol Based Method*: Another data detection method is based on comparing the received payload signals to the 16 reference symbols of the preamble as a combined "16-QAM" stream. Both RX-antennas are used for

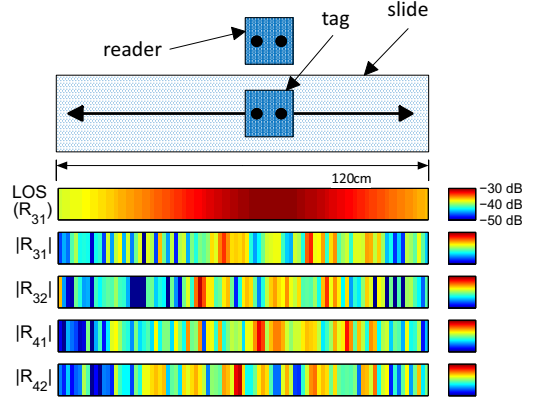


Fig. 7. Measured channel coefficients

a SNR-weighted combined decision. Since for distinct channel realizations some constellation points may overlap, detection is not possible in any case resulting in a degraded SER performance.

## IV. MEASUREMENT RESULTS

### A. Channel

Fig. 7 shows the magnitude of the channel coefficients calculated as described in Sec. III-A for a multitude of channel realizations in a spatial grid of  $\lambda/4$ . Additionally, the LOS share of  $R_{31}$  is estimated by using far field free space path loss assumptions for comparison. Due to the multi-path environment, an intense small scale fading based on multiple NLOS propagation paths superimposed by the LOS path is present, which may be modeled by a Rician distribution with varying power in the LOS path. Fig. 8 additionally shows the corresponding cumulative distribution function (CDF), illustrating that all coefficients are similarly distributed.

### B. Channel Capacity

Fig. 9 depicts the channel capacity as calculated using (3) and measured CSI from Sec. IV-A for different antenna scenarios (all channels normalized by the averaged magnitude of all coefficients involved in order to obtain a mean SNR  $\rho = 10$  dB). For comparison, Fig. 10 shows the simulated capacity for these scenarios, when Rayleigh fading (solely NLOS share) is assumed (10000 realizations, see [18]). More antennas on each side provide more capacity, whereas, however, more transponder antennas are superior to, e.g., more RX-antennas, due to the transponder being a link between forward and backward channel similar to a keyhole.

### C. Symbol Error Ratios for Spatial Multiplexing

For each channel realization, backscatter transmission of two spatially multiplexed symbol streams is assessed. Fig. 11 verifies the feasibility of separating both streams (unequal SNR) with zero forcing for an exemplary measurement. The constellations slightly differ from each other due to the modulator fabrication process. Fig. 12 compares both methods from Sec. III-D for two tag scattering antennas ( $L = 2$ ) in addition to one stream with one scattering antenna ( $L = 1$ ) in terms

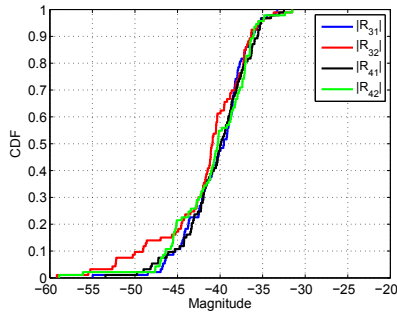


Fig. 8. Channel coefficients

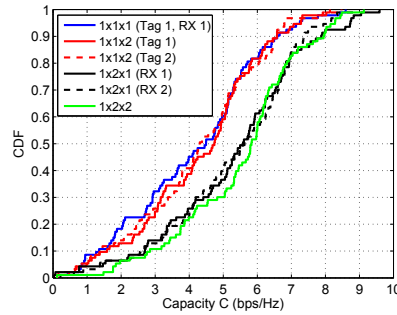


Fig. 9. Capacity

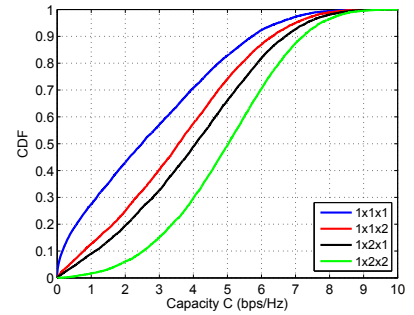


Fig. 10. Capacity, Rayleigh fading

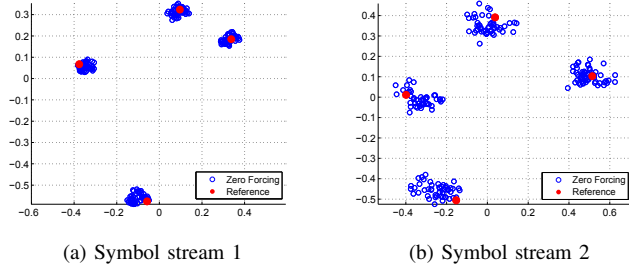


Fig. 11. Separated payload symbols using zero forcing

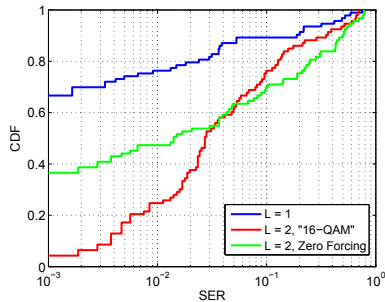


Fig. 12. Symbol error ratios

of the SER. Obviously, one stream shows best performance compared to two streams sharing the spectrum. Using CSI for zero forcing outperforms the reference symbol based method.

## V. CONCLUSION

In this contribution multi-antenna backscatter measurements at 5.8 GHz with up to two scatter and two receive antennas in a multi-path environment are presented. Results for the individual sub-channels of forward and backward link in various realizations are shown, allowing for an investigation of the backscatter link capacity. Additionally, the symbol error ratios for spatial multiplexing backscatter transmission are assessed.

## ACKNOWLEDGMENT

This work was supported by Deutsche Forschungsgemeinschaft, Grant GE 1667/3-1.

## REFERENCES

[1] D. Dobkin, *The RF in RFID*. Elsevier, 2007.  
 [2] G. Marrocco, "Pervasive electromagnetics: sensing paradigms by passive rfid technology," *IEEE Wireless Communications*, vol. 17, no. 6, pp. 10–17, Dec. 2010.

[3] H. N. Schwerdt, F. A. Miranda, and J. Chae, "Analysis of electromagnetic fields induced in operation of a wireless fully passive backscattering neurorecording microsystem in emulated human head tissue," *IEEE Transactions on Microwave Theory and Techniques*, vol. 61, no. 5, pp. 2170–2176, May 2013.  
 [4] R. Correia, N. B. Carvalho, and S. Kawasaki, "Continuously power delivering for passive backscatter wireless sensor networks," *IEEE Transactions on Microwave Theory and Techniques*, vol. 64, no. 11, pp. 3723–3731, Nov. 2016.  
 [5] J. D. Griffin and G. D. Durgin, "Gains for rf tags using multiple antennas," *IEEE Transactions on Antennas and Propagation*, vol. 56, no. 2, pp. 563–570, Feb. 2008.  
 [6] M. Ingram, M. Demirkol, and D. Kim, "Transmit diversity and spatial multiplexing for rf links using modulated backscatter," in *Proc. International Symposium on Signals, Systems, and Electronics (ISSSE)*, July 2001.  
 [7] C. He, X. Chen, Z. J. Wang, and W. Su, "On the performance of mimo rfid backscattering channels," *EURASIP Journal on Wireless Communications and Networking*, vol. 2012, no. 1, pp. 357–371, 2012.  
 [8] G. Yang, C. K. Ho, and Y. L. Guan, "Multi-antenna wireless energy transfer for backscatter communication systems," *IEEE Journal on Selected Areas in Communications*, vol. 33, no. 12, pp. 2974–2987, Dec. 2015.  
 [9] F. Zheng and T. Kaiser, "On the transmit signal design at the reader for rfid mimo systems," in *Proc. Fourth International EURASIP Workshop on RFID Technology (EURFID)*, Sept. 2012, pp. 59–64.  
 [10] D. Kim, M. A. Ingram, and W. W. Smith, "Measurements of small-scale fading and path loss for long range rf tags," *IEEE Transactions on Antennas and Propagation*, vol. 51, no. 8, pp. 1740–1749, Aug. 2003.  
 [11] A. Lazaro, D. Girbau, and D. Salinas, "Radio link budgets for uhf rfid on multipath environments," *IEEE Transactions on Antennas and Propagation*, vol. 57, no. 4, pp. 1241–1251, Apr. 2009.  
 [12] J. D. Griffin and G. D. Durgin, "Multipath fading measurements at 5.8 ghz for backscatter tags with multiple antennas," *IEEE Transactions on Antennas and Propagation*, vol. 58, no. 11, pp. 3693–3700, Nov. 2010.  
 [13] D. Arnitz, U. Muehlmann, and K. Witrisal, "Wideband characterization of backscatter channels: Derivations and theoretical background," *IEEE Transactions on Antennas and Propagation*, vol. 60, no. 1, pp. 257–266, Jan. 2012.  
 [14] J. Kaitovic, M. Limko, R. Langwieser, and M. Rupp, "Channel estimation in tag collision scenarios," in *Proc. IEEE International Conference on RFID (RFID)*, Apr. 2012, pp. 74–80.  
 [15] E. Denicke, M. Henning, H. Rabe, and B. Geck, "The application of multiport theory for mimo rfid backscatter channel measurements," in *Proc. 42nd European Microwave Conference (EuMC)*, Oct. 2012, pp. 522–525.  
 [16] E. Denicke, D. Härke, and B. Geck, "Investigating multi-antenna rfid systems by means of time-varying scattering parameters," in *Proc. 7th European Conference on Antennas and Propagation (EuCAP)*, Apr. 2013, pp. 3314–3318.  
 [17] A. Rumiantsev and N. Ridler, "Vna calibration," *IEEE Microwave Magazine*, vol. 9, no. 3, pp. 86–99, June 2008.  
 [18] E. Denicke and B. Geck, "A network model for evaluating mimo backscatter systems considering mutual coupling," in *Proc. 8th German Microwave Conference (GeMiC)*, Mar. 2014.